HHS Public Access

Author manuscript

Neurobiol Dis. Author manuscript; available in PMC 2022 July 20.

Published in final edited form as:

Neurobiol Dis. 2022 July ; 169: 105719. doi:10.1016/j.nbd.2022.105719.

Human IPSC 3D brain model as a tool to study chemical-induced dopaminergic neuronal toxicity

David Pamies[a,e,1,*], **Daphne Wiersma**[a,1], **Moriah E. Katt**[b,f], **Liang Zhao**[a,c], **Johannes Burtscher**[d,e], **Georgina Harris**[a], **Lena Smirnova**[a], **Peter C. Searson**[b,f], **Thomas Hartung**[a,g], **Helena T. Hogberg**[a]

[a]Center for Alternative to Animal Testing, Johns Hopkins University, 615 North Wolfe St., Baltimore, MD 21205, United States of America

[b]Department of Materials Science and Engineering, Johns Hopkins University, 3400 North Charles Street, Baltimore, MD 21218, United States of America

[c]Bloomberg-Kimmel Institute for Cancer Immunotherapy, Johns Hopkins School of Medicine, Baltimore, MD 21287, United States of America

[d]Institute of Sport Sciences, University of Lausanne, CH-1015 Lausanne, Switzerland

[e]Department of Biomedical Sciences, University of Lausanne, CH-1015 Lausanne, Switzerland

[f]Institute of Nanobiotechnology, 100 Croft Hall, Johns Hopkins University, 3400 North Charles Street, Baltimore, MD 21218, United States of America

[g]CAAT-Europe, University of Konstanz, Universitätstsr. 10, 78464 Konstanz, Germany

Abstract

Oxidative stress is caused by an imbalance between the generation and detoxification of reactive oxygen and nitrogen species (ROS/RNS). This imbalance plays an important role in brain aging and age-related neurodegenerative diseases. In the context of Parkinson's disease (PD), the sensitivity of dopaminergic neurons in the *substantia nigra pars compacta* to oxidative stress is considered a key factor of PD pathogenesis. Here we study the effect of different oxidative

*Corresponding author. david.pamies@unil.ch (D. Pamies).

[1]Both authors contributed equally to this work

CRediT authorship contribution statement

David Pamies: Investigation, Formal analysis, Data curation, Writing – original draft, Writing – review & editing. **Daphne Wiersma:** Investigation, Formal analysis, Data curation. **Moriah E. Katt:** Investigation, Formal analysis, Data curation, Supervision. **Liang Zhong:** Investigation, Formal analysis, Data curation. **Johannes Burtscher:** Writing – original draft, Writing – review & editing. **Georgina Harris:** Investigation, Formal analysis, Data curation, Writing – review & editing, Supervision. **Lena Smirnova:** Writing – review & editing, Supervision. **Peter C. Searson:** Supervision. **Thomas Hartung:** Writing – review & editing, Funding acquisition. **Helena T. Hogberg:** Conceptualization.

Declaration of Competing Interest

Thomas Hartung, Helena Hogberg and David Pamies are named inventors on a patent by Johns Hopkins University on the production of mini-brains (aka BrainSpheres), which is licensed to AxoSim, New Orleans, LA, USA. They and Lena Smirnova consult AxoSim and Thomas Hartung and Helena Hogberg are shareholders. Thomas Hartung consults AstraZeneca, American Type Culture Collection (ATCC), InSphero and Apellis Pharmaceuticals on Microphysiological Systems.

Appendix A. Supplementary data

Supplementary data to this article can be found online at https://doi.org/10.1016/j.nbd.2022.105719.

stress-inducing compounds (6-OHDA, MPTP or MPP^+) on the population of dopaminergic neurons in an iPSC-derived human brain 3D model (aka BrainSpheres). Treatment with 6-OHDA, MPTP or MPP^+ at 4 weeks of differentiation disrupted the dopaminergic neuronal phenotype in BrainSpheres at (50, 5000, 1000 μM respectively). 6-OHDA increased ROS production and decreased mitochondrial function most efficiently. It further induced the greatest changes in gene expression and metabolites related to oxidative stress and mitochondrial dysfunction. Co-culturing BrainSpheres with an endothelial barrier using a transwell system allowed the assessment of differential penetration capacities of the tested compounds and the damage they caused in the dopaminergic neurons within the BrainSpheres In conclusion, treatment with compounds known to induce PD-like phenotypes *in vivo* caused molecular deficits and loss of dopaminergic neurons in the BrainSphere model. This approach therefore recapitulates common animal models of neurodegenerative processes in PD at similarly high doses. The relevance as tool for drug discovery is discussed.

Keywords

Toxicant-induced Parkinson's disease; Microphysiological system; Organoid; 3d culture; Stem cells; iPSC; MPP^+; MPTP; 6OHDA

1. Introduction

Reactive oxygen species (ROS) are by-products of cellular oxygen metabolism (Sies et al., 2022; Halliwell, 1991). They play an important role in different physiological processes and cellular signaling (*e.g.* apoptosis, autophagy, immunological defense, proliferation, differentiation, morphogenesis) (Covarrubias et al., 2008) but are also hazardous to cells by triggering oxidative stress and damage to biomolecules (for recent reviews see (Sies and Jones, 2020; Sies et al., 2022)). Cells therefore possess various mechanisms, such as enzymatic and non-enzymatic antioxidants, to protect themselves against ROS (Covarrubias et al., 2008). A prominent example is glutathione (GSH) that is the most important non-enzymatic, hydrophilic antioxidant (Aquilano et al., 2014). However, disturbance in the balance between pro- and antioxidant mechanisms are involved in numerous pathologies, including neurological diseases and especially aging-related ones. Among these pathologies is Parkinson's disease (PD), a predominantly sporadic neurodegenerative disease, with aging being the main risk factor to develop this illness (Hou et al., 2019). Dopaminergic neurons in the *substantia nigra pars compacta* (SNpc) are especially vulnerable in PD (Gonzalez-Rodriguez et al., 2020) and their loss causes a lack of dopamine (DA) in the striatum (Lee et al., 1994; Hirsch et al., 1988). These reduced DA levels eventually cause the characteristic motor symptoms of PD (Blum et al., 2001). However, PD is characterized by widespread other brain pathologies, including protein aggregation (Lashuel et al., 2013), metabolic deficits (Monzio Compagnoni et al., 2020) and neurodegeneration also of other neuronal populations (Paredes-Rodriguez et al., 2020; Blesa et al., 2022), and is often associated with various non-motor symptoms (Marinus et al., 2018; Blesa et al., 2022). Among those, cognitive impairments, hallucinations, depression and apathy are particularly prominent (Marinus et al., 2018). Motor symptoms usually manifest first after 50–80% of the dopaminergic neurons in the SNpc are lost, in which case the disease state is strongly

advanced (Blum et al., 2001; Dauer and Przedborski, 2003). Despite much ongoing research on the molecular factors that drive PD progression, the mechanistic understanding of the selective vulnerability of dopaminergic neurons is still poor. Dopaminergic neurons in general exhibit high basal levels of ROS, based on their metabolic peculiarities, namely enzymatic catabolism and neuromelanin production (Gonzalez-Rodriguez et al., 2020; Wong and Krainc, 2017) that likely contribute to their vulnerability (Hirsch et al., 1997). A better understanding of the mechanisms leading to neurodegeneration of dopaminergic neurons in PD requires new *in-vitro* and *in-vivo* models that are relevant for the human disease. Neurotoxin models of PD are very commonly used; we showed earlier how publications of PD using animal models have almost tripled from the mid 80ies (Daneshian et al., 2015) over three decades with for example increases in the use if MPTP as a PD-causing agent. The clinical success of the resulting drug candidates was limited with an analysis of 357 clinical trials since 1999 showing the exclusive approval of compounds in a narrow range of symptomatic treatment for PD (Boucherie et al., 2021). This has led to some discussion of the value of these models, for example rodents (Vingill et al., 2018; Faivre et al., 2019). Some authors (Bezard et al., 2013) highlight the superior translational relevance of monkey models but also powerful *in vitro* alternatives are becoming increasingly available. We thus aimed to explore, if emerging human brain 3D models have the potential to transform PD in vitro models. 3D IPSC-derived model derived from human cells may better reflect processes of human brain aging, recapitulating parts of the complex diversity and inter-connectivity in the human brain (Aguado and Wolvetang, 2022).

In the past years, we have developed a 3D human induced pluripotent stem cells (iPSC) brain model (BrainSphere) that recapitulates many aspects of the human brain (Pamies et al., 2016). The model contains a mixed population of neurons, astrocytes and oligodendrocytes that exhibit myelinated axons and spontaneous electrical activity [11]. The BrainSphere model has been shown to be very well suited to study neurotoxicity and developmental neurotoxicity, gene environmental interactions (Zhong et al., 2020; Pamies et al., 2018; Modafferi et al., 2021; Chesnut et al., 2021), as well as for other applications (Plummer et al., 2019; Zhou et al., 2021; Zander et al., 2017). The objective of this study was to determine if this model also can reproduce neurodegenerative processes, such as loss of dopaminergic neurons due to increased ROS production. The use of human iPSCs makes the model more relevant for human disease, which may be a major advantage for translational drug-discovery. Moreover, this approach enables studies of gene-environment interactions on a personalized level using patients iPSCs and thus may promote precision medicine for PD.

As an important validation to assess the suitability of our model as a model for PD, we selected 3 compounds known to increase ROS production and to cause dopaminergic neuron loss (Blum et al., 2001): 6-hydroxydopamine (6-OHDA), 1-methyl-4-phenyl-1,2,3,6-tetrahydropyridine (MPTP) and its active metabolite 1-methyl-4-phenylpyridinium (MPP^+). All of these compounds induce parkinsonism and thus have extensively been used to model PD (Tieu, 2011). 6-OHDA is known to accumulate in the cytosol and promote formation of ROS, especially hydrogen peroxide, inducing dopaminergic neuronal death in less than 24 h (Jeon et al., 1995). Due to its hydrophilic nature, 6-OHDA does not readily cross the blood brain barrier (BBB) (Jagmag et al., 2016), however, there is evidence that it is able to disrupt the BBB, altering its permeability (Carvey et al., 2005). MPTP may be

accidentally produced during the manufacture of 1-methyl-4-phenyl-4-propionoxypiperidine (MPPP, Desmethylprodine), a synthetic opioid drug, and was found to induce parkinsonism in illicit drug users. MPTP is the neurotoxic precursor of MPP^+, that has been shown to preferentially damage dopaminergic neurons. The conversion from MPTP to MPP^+ requires glial monoamine oxidase B (Jagmag et al., 2016). MPP^+ is taken up by dopaminergic neurons, where it inhibits the mitochondrial electron transport chain and produces oxidative stress (Blum et al., 2001). Toxicant-based models of PD (6-OHDA and MPP^+, rotenone and paraquat) are among the most widely used animal models of PD (Le et al., 2014), however, their translation potential to clinics has been poor. These models are not suitable to model PD pathogenesis, but they are useful to study neuroprotective strategies and potentially develop disease-modifying strategies (Le et al., 2014; Kalia et al., 2015). Here we introduce a human model as an alternative to chemical-induced PD animal models. Exposure of BrainSpheres to those chemicals (6-OHDA, MPTP and MPP^+) resulted in selective loss of dopaminergic neurons, recapitulating the vulnerability of these cells in PD. We observed a clear change in REDOX homeostasis confirming the central role of oxidative stress for the detrimental effects of these compounds.

2. Materials and methods

All the experiments have been made under good cell culture practice (Pamies et al., 2022).

2.1. Compounds

6-OHDA, MPTP, and MPP^+ were purchased from Sigma-Aldrich (St. Louis, MO). All stocks were prepared in 1× PBS at concentrations of 100 mM for 6-OHDA and MPTP and 30 mM for MPP^+ and stored at −20 °C.

2.2. Neural progenitor cell maintainance

IPSC-derived neural progenitor cells (NPC) were kindly provided by Professor Hongjun Song's lab within our joint NIH NCATS project (Pamies et al., 2016). NPCs were derived from C1 (CRL-2097) fibroblasts purchased from ATCC. Differentiation from iPSC to NPC has been previously described (Wen et al., 2014). NPCs were cultured in poly-lornithine and laminin-coated 175 cm^2 flasks in NPC medium (KnockOut DMEM/F12 [Gibco] supplemented with 2% Stempro® [Gibco], 1% Glutamax [Gibco], 1% Pen-strep [Gibco], 20 ng/ml endothelial growth factor [Gibco], and 20 ng/ml basic fibroblast growth factor [Gibco]). Half of the media was exchanged every day. Cultures were maintained at 37 °C in a humidified atmosphere of 5.0% CO_2. Passages 17–24 were used for neural differentiation.

2.3. BrainSpheres neural differentiation

BrainSpheres were generated as previously described (Pamies et al., 2016). Briefly, at 90% confluence, NPCs were detached mechanically. 2×10^6 cells per well were plated in 2 ml of medium in non-coated 6 wellplates. Cells were kept under constant gyratory shaking (88 rpm, 19 mm orbit) by using a MaxQ™ 2000 CO2 [ThermoFisher] plate shaker in NPC expanding medium for two days, then the medium was changed to differentiation medium (Neurobasal® electro Medium [Gibco] supplemented with 2% B-27® Electrophysiology [Gibco], 1% glutamax [Gibco], 10 ng/ml human recombinant GDNF [Gemini Bio Products],

10 ng/ml human recombinant BDNF [Gemini Bio Products]. Cultures were maintained further under gyratory shaking (5.0% CO_2, 37 °C, 88 rpm) for up to 4 weeks. Differentiation medium was exchanged every 2–3 days.

2.4. Brain microvascular endothelial cells

To mimic the blood-brain barrier, human brain microvascular endothelial cells (hBMECs) were derived from iPSCs. The hBMECs were maintained and derived from the BC1 iPSC line (Chou et al., 2011) as previously described (Katt et al., 2016). Stem cells were maintained in TeSR-E8 medium [Stem Cell Technologies] in tissue culture flasks [BD Falcon] coated with growth factor-reduced Matrigel [Corning]. Cells were passaged using Accutase [Life Technologies] with the addition of 10 μM y-27,632 [ATCC] to the culture media. For the differentiation, cells were switched to unconditioned media (DMEM/F12 [Life Technologies] supplemented with 20% KOSR [Life Technologies], 1% nonessential amino acids [Life Technologies], 0.5% L-glutamine [Sigma], and 0.836 μM beta-mercaptoethanol [Life Technologies]) for 6 days followed by 2 days of endothelial cell media (endothelial cell serum-free media [Life Technologies] supplemented with 1% human platelet-poor derived serum [Sigma], 2 ng mL-1 bFGF [R&D Systems], and 10 μM retinoic acid [Sigma]). Cells were then sub-cultured in 6.4 mm transwell inserts with polyester membranes with a pore size of 0.4 μm [Corning] coated with 50 μg/mL collagen IV [Sigma] and fibronectin [Sigma] overnight. Cells were seeded at a density of 1×10^6 cells/ml in the endothelial cell medium. Media was changed after 24 h to remove non-adherent cells and every 48 h thereafter. To mimic blood-brain barrier transport, BrainSpheres differentiated for 4 weeks were added to the lower chamber of the transwell 2 days after the endothelial cells were seeded on the membrane. Transendothelial Electrical Resistance (TEER) measurements were used to assess barrier function, see below.

2.5. BrainSpheres treatment with PD-inducing chemicals

At 4 weeks of differentiation, the medium was replaced with 2 ml of fresh differentiation medium (Fig. 1A). Subsequently, BrainSpheres were exposed for 24 h to compounds known to induce ROS production (6-OHDA, MPTP, or MPP^+) at a wide range of concentrations (10 μM – 5000 μM) (Fig. 1A). For the ROS assay, differentiation medium Neurobasal® electro medium [Gibco] was replaced with Neurobasal medium without phenol red [Gibco]. The 6-wells plates were returned to the incubator with gyratory shaking (5.0% CO_2, 37 °C) for 24 h. After exposure, multiple assays were performed as described below. In addition, in order to study the recovery of the cells, different treatments were removed from the media, BrainSpheres were washed 3 times with PBS, and then cultured for 5 days before collection.

2.6. Resazurin assay

As a measurement for cell viability, the resazurin (7-Hydroxy-3*H*-phenoxazin-3-one 10-oxide) reduction assay was performed (protocol adapted (O'Brien and Pognan, 2001)). After 21 h of exposure to selected chemicals (6-OHDA, MPP^+ and MPTP), resazurin was added to each well (25 μg/ml final concentration), and BrainSpheres were incubated for 3 h under gyratory shaking (5.0% CO_2, 37 °C, 88 rpm), yielding a total of 24 h of exposure to test compounds. A volume of 100 μl medium from each sample was transferred into 96-wells

plates, and fluorescence was measured in a CytoFluor multi-well plate reader series 4000 [Perseptive Biosystems] at 530/590 nm excitation/emission.

2.7. ROS assay

To quantify oxidative stress in the BrainSpheres, the OxiSelect *in vitro* ROS/RNS assay kit [Cell Biolabs Inc., San Diego, CA, USA] was used. This kit is based on the oxidation of DCFH by ROS into the fluorescent form 2′, 7′-dichlorodihydrofluorescin (DCF). The fluorescence intensity is proportional to the ROS levels within the samples. After 24 h exposure, 50 µl medium samples were collected in 96-wells plates and incubated with 50 µl Catalyst solution (Catalyst 1:250 in PBS) for 5 min at room temperature. Thereafter, 100 µl of DCFH solution DCF-Dioxy solution (DCF-DiOxyQ 1:5 in priming reagent) 1:40 in (1×) stabilization solution (stabilization solution 10 × 1:10 in deionized water) was added and the plate was incubated in the dark at room temperature for 45 min. Fluorescence was then measured in a CytoFluor multi-well plate reader series 4000 [Perseptive Biosystems] at 485/530 nm excitation/emission.

2.8. Mitotracker

To assess mitochondrial membrane potential, MitoTracker® Red CMXRos [Invitrogen] was used. Mitochondrial function can be determined by decreased fluorescent intensity. In the last 30 min of the 24 h exposure, the BrainSpheres were transferred into 12-wells plates with 500 µl medium and 2 µM MitoTracker® per well and were incubated for 30 min (5.0% CO_2, 37 °C). Subsequently, the cells were fixed in 4% paraformaldehyde for 30 min at room temperature and washed once with PBS. BrainSpheres were then transferred onto microscope glass slides and mounted with ‘Immuno mount’ [Thermo Fisher Scientific]. Fluorescence intensity images were taken with an Olympus BX60 microscope [Olympus, Center Valley, PA, USA], connected to Qimaging Retiga Exi [Qimaging, Surrey, BC, Canada] camera and Image-Pro Plus software [v7.0, Media Cybernetics Inc., Rockville, MD, USA] and further analyzed with ImageJ software [v. 1.48, NIH, Baltimore, MD, USA].

2.9. Transendothelial electrical resistance recording

Transendothelial Electrical Resistance (TEER) was measured on day 2 after seeding the iPSC-derived hBMECs onto the transwell inserts using an EVOM2 and STX2 probe [World Precision Instruments]. Reported TEER values were corrected for measurements in blank wells (no cells), typically about 40 Ω cm^2.

2.10. Endothelial cell area calculation

Cell area was measured by tracing individual endothelial cells from ZO-1 immunofluorescence staining using ImageJ with the Bio-Formats plug in. A minimum of 20 cells were measured for each condition.

2.11. Immunocytochemistry

To characterize the neuronal population of the model, immunocytochemistry was performed. After 24 h exposure, the BrainSpheres were collected and fixed in paraformaldehyde (4%) for 30 min at room temperature. Subsequently, the BrainSpheres were washed

twice with PBS (1×) and incubated with blocking solution (10% goat serum, 1% BSA, 0.15% saponin in PBS) at 4 °C for 1 h. The BrainSpheres were washed with washing solution (1% BSA, 0.15% saponin in PBS), and incubated overnight at 4 °C with primary antibodies: anti- Calbindin 1 (CALB1) (1:200, for dopaminergic neurons) [ABclonal], anti-Potassium Inwardly Rectifying Channel Subfamily J Member 6 (KCNJ6) (1:200, for dopaminergic neurons)[ABclonal], anti-tyrosine hydroxylase (TH) (1:100, for dopaminergic neurons)[Millipore], anti-NF200 (1:200, neurofilament for all neurons) [Sigma] and anti-ZO-1 (1:200, endothelial tight junctions) [Life Technologies] diluted in blocking solution. The next day the BrainSpheres were washed twice with washing solution and incubated with the secondary antibody 568-Alexa anti-rabbit or 488-Alexa anti-mouse both 1:200 diluted in blocking solution for 6 h at room temperature protected from light. Thereafter, BrainSpheres were washed twice again with washing solution. Nuclei were stained with Hoechst 33342, diluted 1: 10,000 in PBS for 1 h. The BrainSpheres were transferred to microscope glass slides and mounted with 'Immuno mount' and imaged with a confocal microscope Zeiss LSM 510 Confocal III (Zeiss) with a 20× and 63× objectives.

2.12. RNA extraction and cDNA generation

BrainSpheres were exposed for 24 h to 6-OHDA, MPTP, or MPP^+. After the cell viability assay the BrainSpheres were collected and washed with PBS (1×). Total RNA was extracted from the BrainSpheres with the mirVana RNA isolation kit [Ambion Life Technologies, Grand Island, NY, USA] according to the manufacturer's protocol. Prior cDNA syntheses, the concentration and purity of the RNA was determined with NanoDrop [Thermo Scientific]. 1 µg of RNA was was reverse transcribed using M-MLV Reverse Transcriptase and Random Hexamer primers [Promega]. Briefly, mastermix 1 (1.25 µl dNTP, 0.5 µl random primers) was added to RNA and the samples were incubated in Techne® Endurance TC-312 Thermal Cycler [Techne Inc., Burlington, NJ, USA] for 5 min at 65 °C following 5 min at 4 °C. Subsequently, mastermix 2 (4 µl M-MLV buffer, 1 µl M-MLV enzyme, and 1 µl RNase OUT) was added and samples were incubated for 10 min at 25 °C, 1 h at 37 °C, and 15 min at 70 °C. cDNA samples were stored at −20 °C until real-time quantitative Polymerase Chain Reaction (RT-qPCR) was performed.

2.13. RT-qPCR

cDNA samples (1 µl) were distributed in the RT-qPCR MicroAmp Fast Optical 96-well reaction plates [TermoFisher] and combined with 0.75 µl Taqman gene expression assay [Applied Biosystems], 12.5 µl TaqMan Fast Advanced Master Mix [Applied Biosystems], and 9.25 µl DNA/RNA/RNase free water, following the TaqMan gene expression assay protocol [Thermofisher]. RT-PCR was performed in 7500 Fast Real-Time PCR System [Applied Biosystems] according to the Applied Biosystems protocol (holding stage of 10 min at 95 °C, following 40 cycles of 10 s at 95 °C and 30 s at 60 °C). The relative gene expression was normalized to the housekeeping gene ß-Actin. Primers are listed in Table 1.

2.14. Metabolomics

Sample preparation and LC-MS metabolomics analysis has been previously described (Krug et al., 2014). Briefly, two experiments with 4 biological replicates were performed. For each sample, 625 µl of media was added to 375 µl acetonitrile (ACN) resulting in a 40%

acetonitrile solution. Samples were centrifuged at 14,000 ×*g* for 10 min to precipitate the proteins. A volume of 250 µl of the supernatant was mixed with 250 µL of water and then added to a 3 kDa molecular weight cut-off filter spin column (Microcon YM-3 Centrifugal Filter [Millipore]). After filtering, (Maertens et al., 2017) samples were dried with a vacuum evaporation system. The dried samples were reconstituted in 100 µl of 60% methanol with 0.1% –formic acid and clarified by centrifugation at 14,000 ×*g* for 5 min. The cleared samples were transferred to plastic vials for LC-MS measurements. Targeted LC-MS analysis were performed on an Agilent 6490 triple quadropole LC-MS/MS system with iFunnel and Jet-Stream® technology [Agilent] equipped with an Agilent 1260 infinity pump and autosampler. MS was operated in positive and negative switching mode (unit resolution) with all analytes monitored by multiple reaction monitoring (MRM). Compound identity was confirmed by comparison to the retention times of pure standards using the MassHunter Acquisition software [Agilent] and processed as previous described. The optimized operating ESI conditions were: gas temperature 230 °C; gas flow 15 l/min; nebulizer pressure 40 psi; sheath gas temperature 350 °C and sheath gas flow 12 l/min. Capillary voltages were optimized to 2500 V with nozzle voltages of 1500 V in positive mode, and 4000 V with nozzle voltages of 2000 V in negative mode. All data processing was performed with the Agilent Mass Hunter Quantitative Analysis software package.

2.15. Statistical analysis

For all statistical comparisons, the data were normalized to vehicle treated controls and compared by non-parametric One-Way ANOVA followed by Kruskal–Wallis multiple comparison H tests (GraphPad Prism 8).

3. Results

3.1. BrainSphers shows dopaminergic neurons expression

Previous results have shown the expression of dopaminergic neurons in BrainSpheres after 8 weeks of differentiation (Pamies et al., 2016). In addition, expression of tyrosine hydroxylase (TH) gene has shown to be expressed at very early stage of differentiation (Pamies et al., 2016). In order to ensure enough maturation for the experiments, BrainSpheres differentiated for 4 weeks were fixed, and staining for neuronal marker (BTUBII), dopaminergic neurons markers (CALB1 and KCNJ6), astrocyte marker (GFAP) and oligodendrocytes marker (O4) (Fig. 1B). Data shows expression of all these markers (Fig. 1B), indicating the presence of dopaminergic neurons and other brain cell types.

3.2. Cytotoxic effects of 6-OHDA, MPTP and MPP^+ in 4 weeks old BrainSpheres

To study the cytotoxic effects of 6-OHDA, MPTP and MPP^+, BrainSpheres were cultured for 4 weeks, and were exposed to different concentrations of the chemicals for 24 h. Viability was analyzed by the resazurin assay (Fig. 2A). All three compounds significantly reduced cell viability in a concentration-dependent manner. 6-OHDA was the most potent with the strongest decrease of viability at 1000 µM. 6-OHDA reduced viability to 39 ± 4% and 29 ± 2% of control at 1000 µM and 5000 µM, respectively. MPTP significantly decreased cell viability at 5000 µM (39 ± 3% of control). MPP^+ showed statistically significant decrease of viability at 1000 µM and 5000 µM (64 ± 11% and 55 ± 17%

of control, respectively). Quantifications in the graphs (Fig. 2A) were obtained from 3 independent experiments, each comprising 3–6 biological replicates. Caspase activation was also performed; however results were difficult to interpret (supplementary material 1).

3.3. Reduction in mitochondrial membrane potential correlates with cytotoxicity

The compounds selected for this study are known to induce mitochondrial dysfunction, therefore, Mitotracker was used to quantify mitochondrial functionality in the BrainSpheres exposed to the test compounds. All compounds reduced mitochondrial membrane potential in a concentration-dependent manner as measured by decreased fluorescence intensity normalized to the area of a sphere (Fig. 2B). 6-OHDA was the most potent compound, showing already statistically significant decrease of mitochondrial function to 61 ± 20% of control at 100 μM and maximum reduction at 5000 μM (2 ± 8% of control; $p < 0.01$). MPTP showed significantly decreased mitochondrial function only at the highest measured concentration, 5000 μM (MPTP 67 ± 5% of control). In the case of MPP^+, 500 μM lead to statistically significant decrease on mitochondrial function (70 ± 3% of control). Overall, 6-OHDA- and MPP^+-induced mitochondrial dysfunction was captured at lower concentrations than reduced viability. On the contrary, MPTP only showed mitochondrial function disruption at cytotoxic concentrations. Quantifications in the graphs (Fig. 2B) were obtained from 3 independent experiments, each comprising at least 5 biological replicates.

3.4. Reactive oxygen species after exposure to 6-OHDA, MPTP and MPP^+

One of the pivotal mechanisms of mitochondria-dependent cell death is oxidative stress. Therefore, we assessed levels of ROS after 24 h exposure to 6-OHDA, MPTP and MPP^+. In this assay, the generation of ROS is proportional to the fluorescence intensity measured in the supernatant. ROS production was significantly changed only at cytotoxic concentrations for all three compounds. It was increased by 6-OHDA at concentrations of 500 μM (177 ± 52%; $p < 0.005$), 1000 μM (214 ± 54%; $p < 0.0001$) and 5000 μM (237 ± 69%; $p < 0.0001$). For MPTP, a significant increase in ROS production was only observed at the two highest concentrations, 1000 μM (126 ± 27%; $p < 0.05$) and 5000 μM (131 ± 11%; $p < 0.005$). In contrast, in MPP^+-treated BrainSpheres, a statistically significant reduction in ROS was detected at 1000 μM (75 ± 11%; $p < 0.005$) and 5000 μM (63 ± 12%; $p < 0.0001$). Quantifications in the graphs (Fig. 2C) were obtained from 3 independent experiments, each comprising at least 3 biological replicates.

3.5. Immunocytochemistry reveals specific morphological alterations of dopaminergic neurons at sub-cytotoxic concentrations

Upon treatment, the neuronal population was characterized by immunocytochemistry. To assess, whether the dopaminergic neurons were more sensitive to the selected chemicals than other neuronal types, we performed immunocytochemistry and confocal image analysis for the dopaminergic marker TH and the axonal marker NF200 (Fig. 3). The dopaminergic vulnerability was rated based on the morphological alterations in TH^+ and $NF200^+$ cells independently at different concentrations (Table 2). Morphological changes in the dopaminergic neurons (compromised integrity of somata and neurite loss) were observed after exposure to 1000 μM MPP^+, with neurofilament being affected only at 5000 μM. MPTP clearly affected the integrity specifically of dopaminergic neurons at 5000 μM, while

at this concentration no neuronal damage was observed by immunocytochemistry. 6-OHDA induced the most substantial effects and compromised dopaminergic morphology already at non-cytotoxic concentrations of 50–100 μM, whereas the neurofilament staining appeared normal up to a concentration of 500 μM and was perturbed only at highest concertation tested in this assay (1000 μM). Both MPP+ and MPTP altered TH^+ cells only at cytotoxic concentrations (resazurin assay) and preceded compromised $NF200^+$ at only slightly lower concentrations. 6-OHDA, on the other hand, exhibited the clearest selective effects on TH-positive cells.

3.6. Expression of genes involved in oxidative stress and mitochondrial function was altered after treatment with 6-OHDA, MPTP or MPP^+

For gene expression analysis, chemical concentrations were selected based on the specific phenotype change of dopaminergic neurons (see Table 2): 500 μM 6-OHDA, 5000 μM MPTP, and 1000 μM MPP^+. For 6-OHDA and MPP^+, these concentrations did not induce statistically significant changes in cell viability. However, for MPTP a cytotoxic concentration was selected since no morphologic effects were found at lower concentrations (Fig. 3). Genes related to mitochondrial function, oxidative stress, PD, and markers for dopaminergic neurons were studied. Quantifications in the graphs (Fig. 4) were obtained from 3 independent experiments, each comprising 3 biological replicates.

3.6.1. Genes related to dopaminergic neurons—Genes involved in development and function of dopaminergic neurons were selected to evaluate effects on this specific neuronal population after the exposure. *SLC6A3* encodes for the dopaminergic transporter (DAT), which is responsible for the re-uptake of dopamine from the synaptic cleft by dopaminergic neurons. *KCNJ6* also called G-protein-regulated inward-rectifier potassium channel 2 (*GIRK2*), is a protein that is reported to be expressed in certain dopamine neurons of the substantia nigra (SN) (Reyes et al., 2012) and to be very important for PD. CALB1 is expressed at higher levels in dopamine neurons and is considered a marker for dopaminergic neurons. *TBR1* encodes T-box brain-1 protein, which is essential for neuronal development and axon guidance. *TH* (tyrosine hydroxylase) is the rate-limiting enzyme in the conversion of tyrosine to dopamine. Expression of *TBR1* was significantly up-regulated by 6-OHDA and MPTP (Fig. 4A), while no effect was observed after exposure to MPP^+. Exposure to 6-OHDA also significantly induced expression of *TH and SLC6A3* (Fig. 4A), while expression of KCNJ6 and CALB1 was statistically significant reduced by all the treatments (Fig. 4A) corroborating the effects observed by immunocytochemistry (Fig. 3). The increase in expression of *TH* and *SLC6A3* markers could be a compensatory mechanism of the remaining dopaminergic neurons. MPP^+ and MPTP did not significantly change the expression of *TH and SLC6A3* (Fig. 4A).

3.6.2. Mitochondrial complex I and V genes—6-OHDA, MPTP and MPP^+ were shown to disrupt mitochondrial complex I (Blum et al., 2001). For this reason, genes encoding subunits of mitochondrial complex I, *NDUFA1* and *NDUFB1,* were selected for analysis. In addition, the gene *ATP5O,* a subunit of mitochondrial complex V, the last complex of the respiratory chain in the mitochondria, was evaluated (Fig. 4A). Exposure to 6-OHDA induced a significant increase in the expression of *ATP5O* (Fig. 4A), while

the expressions of complex I subunits were unchanged. None of the compounds altered the *NDUFA1* expression. In contrast, MPTP significant reduced expression levels of *NDUFB1* (Fig. 4A). It is possible that longer exposures (>24 h) are necessary to see strongest changes in gene expression.

3.6.3. Genes involved in cellular defense mechanisms against ROS—The selected compounds are known to induce oxidative stress (Blum et al., 2001). Therefore, genes involved in cellular defense against oxidative stress were evaluated. The *GSTO1* gene encodes for glutathione-S transferase, which is involved in the cellular redox homeostasis. Superoxide dismutase 2 (*SOD2*) is the mitochondrial form of SOD, transforming superoxide to oxygen and hydrogen peroxide. *KEAP1* encodes for kelch-like ECH-associated protein 1, a protein that during normal condition binds and repress the activation of Nuclear factor erythroid 2-related factor 2 (Nrf2). When a cell is experiencing an increase in ROS levels the Nrf2 gets activated and regulates cellular antioxidant responses. Exposure to 6-OHDA caused an increase of ROS (Fig. 2C). In agreement with this observation, real-time qPCR results showed increased expression of *GSTO1 and SOD2* by MPTP and 6-OHDA treatment (Fig. 4A). MPTP also showed increased ROS, which was reflected by increased expression of *KEAP1* and *GSTO1* (Fig. 4A). MPP^+ did not induce ROS production and did not alter the expression of associated genes (Fig. 4A).

3.6.4. Perturbation of extracellular metabolites after 24 h exposure to PD inducing toxicants—Extracellular metabolites were measured in the medium 24 h after exposure. For this experiment, we performed a targeted approach with selected metabolites that have been shown to be involved in oxidative stress, mitochondrial and neuronal function. Moreover, metabolites neurotransmitters and amino acids proposed to be involved in PD pathophysiology, possible biomarkers and treatment targets were measured. Metabolites related to energy metabolism (glucose, adenosine and creatine) were altered after chemical exposure (Fig. 4B). Glucose, the primary source of energy for the cells, is introduced with the cell medium as the principal nutrient for BrainSpheres culture. Exposure to MPP^+ and 6-OHDA decreased extracellular D-glucose in the medium, which may indicate higher consumption by the cells under stress. Creatine, which facilitates recycling of adenosine triphosphate (ATP), was also decreased after treatment with 6-OHDA and MPP^+, suggesting a higher consumption of this metabolite. Adenosine is involved in the ATP cycle and has been suggested to play an important extracellular role in the CNS, by regulating neuronal and glial cell functions (Bjorklund et al., 2008; Fredholm et al., 2005). Adenosine modulates the action of various neurotransmitters, including dopamine and can modulate the interaction of dopamine with their own receptor; moreover, it has been suggested as treatment in PD. Our experiments show that exposure to 6-OHDA and MPTP increased extracellular adenosine (Fig. 4B).

Serotonin or 5-hydroxytryptamine (5-HT) is a monoamine neurotransmitter that is considered a dopaminergic agonist. Serotonin has been related to PD in many studies; however, the association is not clear. Aromatic L-amino acid decarboxylase (AADC)-expressing serotonergic neurons can convert L-DOPA to dopamine (Carlsson et al., 2007). A serotonergic hyper-innervation in the striatum, with the detection of dopamine in

serotonergic varicose fibers, suggesting a compensatory mechanism has been shown (Bedard et al., 2011). There was no significant change in the extracellular levels of serotonin after any of the treatments (Fig. 4B). Mouse studies have revealed decreased D- and L-serine levels in the midbrain correlated with aggravation of PD symptoms, which suggests that serine may participate in PD pathogenesis (Li et al., 2009). In our experiments, none of the treatments showed a significant reduction of extracellular serine (Fig. 4B).

Protein misfolding is thought to be a major contributing factor in a number of neurodegenerative diseases, including PD. Amino acid proline addition or uptake is delayed during *in vitro* and *in vivo* protein aggregation (Yeo et al., 2015). Accordingly, the MPTP mouse model of PD shows an increase in extracellular proline concentrations (Fisher, 2006) that correlates with our finding: statistically significant increase in extracellular proline after exposure to all three compounds (Fig. 4C). Methionine is an essential sulfur-containing amino acid in humans. It has been suggested as a treatment similar to L-DOPA for PD (Meininger et al., 1982). Exposure to MPP^+ and MPTP increased the extracellular levels of methionine (Fig. 4B). Finally, exposure to MPTP also increased the extracellular levels of the neurotransmitter glutamate.

3.6.5. Delayed gene expression responses 5 days after compound washout

—We wanted to study the late effects and possible recovery of the cells after selected chemical exposure. For that, after 24 h of treatment, the compounds were washed out and BrainSpheres were cultured for 5 additional days in fresh medium to allow recovery. BrainSpheres were then collected and analyzed by real-time qPCR (Fig. 4C). Two genes commonly associated with dopaminergic cell loss *TH* and *SNCA,* were studied after 5 days washout. In these experiments, decrease in *TH* expression was observed for all three compounds, however, it was statistically significant only for 6-OHDA. Various mutations of the *SNCA* gene were shown to cause familial forms of PD (Polymeropoulos et al., 1997; Kruger et al., 1998; Zarranz et al., 2004; Singleton et al., 2003; Ibanez et al., 2004). SNCA encodes alpha-synuclein, the main component of a pathological hallmark of PD, *i.e.*, Lewy bodies (Spillantini et al., 1997). However, after wash-out, 6-OHDA showed a statistically significant decrease in expression of *SNCA* (Fig. 4C). Other markers such as the astrocyte marker *GFAP*, the neuronal marker *BTUBIII*, the oligodendrocyte marker *OLIG2* and the oxidative markers *GSTO1* and *SOD2* were also studied after 5 days washout (Fig. 4C). Most of these genes showed no statistically significant changes, indicating that the treatment was affecting specifically dopaminergic cells. However, the *GFAP* marker was significantly decreased in 6-OHDA treated BrainSpheres. In addition, there was a trend of increased *OLIG2* in MPTP- and reduced *OLIG2* in MPP^+-treated cells after the washout, however these changes were not statistically significant. In conclusion, the delayed PCR measurements corroborate that predominantly dopaminergic neurons are affected by the treatment.

3.7. Blood-Brain Barrier incorporation into the BrainSpheres PD model

The blood-brain-barrier (BBB) is a unique biological barrier, providing the interface between the vascular system and the brain. In addition to supplying nutrients for normal brain function, the BBB is responsible for regulating the brain microenvironment by

preventing fluctuations in chemistry, transport of immune cells, and the entry of toxins and pathogens (Wong et al., 2013). Because of its function in restricting entry of small molecules, the BBB is a major bottleneck in delivering drugs and toxicants to the brain. Exposure to 6-OHDA, MPTP and MPP^+ disrupted (dopaminergic) neurons in BrainSpheres (Fig. 3), however, only MPTP of the studied chemicals is able to cross the BBB *in vivo* (Schmidt et al., 1997). Therefore, to assess the role of BBB transport, we developed a transwell-based model where human brain microvascular endothelial cells were seeded on the transwell membrane insert and 4-weeks differentiated BrainSpheres were cultured in the basolateral chamber (Wong et al., 2013).

Chemicals of interest (500 μM 6-OHDA, 5000 μM MPTP or 1000 μM MPP^+) were applied apically. In this approach, the chemicals must be transported across the endothelial monolayer to reach the BrainSpheres. Immunocytochemistry, and TEER measurements were performed after 24 h exposure (Fig. 5A and B).

Immunostaining of BrainSpheres after treatment across the BBB model with 6-ODHA and MPTP revealed a change in morphology of the dopaminergic neurons (Fig. 5A), indicating that these molecules were able to cross the endothelial monolayer at sufficiently high concentrations to induce changes in cell phenotype of dopaminergic neurons in the BrainSpheres. Immunostaining of brain microvascular endothelial cells revealed consistent ZO-1 junctional formation across all conditions. However, with significantly increased cell area after exposure to all compounds compared to the control, indicating possible cell death and monolayer remodeling to compensate.

The average TEER values for derived brain microvascular endothelial cells was 1250 ± 5 Ω x cm^2, consistent with physiological values (Wong et al., 2013). Exposure to MPTP for 24 h did not result in any change in TEER, however, both 6-OHDA and MPP^+ resulted in a statistically significant decrease (Fig. 5D). BBB disruption can result in entry of blood components and lead to changes in permeability, immune cell transport, and trafficking of pathogens into the brain, which ultimately can lead to neuroinflammation, oxidative stress, and neurotoxicity. MPTP results in morphological changes in dopaminergic neurons indicating that it is able to cross the BBB by a transcellular mechanism without inducing disruption of the endothelial layer. In addition to disruption of the dopaminergic cell phenotype, decreased mitochondrial activity was observed in BrainSpheres in response to 6-OHDA and MPTP exposure of the BBB model (Fig. 5D). In conclusion, these experiments showed that a BBB can be added to the model recapitulating the crossing of MPTP *in vivo* and allowing toxicity of the other toxicants only at concentrations toxic to the BBB integrity.

4. Discussion

IPSC-derived 3D models bring a great opportunity to study neurodegenerative diseases (Chang et al., 2020). Some advances in organoid cultures have made the generation of models that better represent human brain possible, although also bring some limitations (Pamies et al., 2020; Pamies and Hartung, 2017). Especially the development of midbrain organoids has the potential to better model Parkinson diseases (Renner et al., 2020; Jo et al., 2016; Fiorenzano et al., 2021). The application of these new models to high throughput

technologies also will facilitate the discovery of new treatments in the future (Renner et al., 2020). In this study we used the human BrainSphere model to study selective vulnerability of dopaminergic neurons to compounds known to induce PD like phenotypes *in vivo*. The model could represent an important complementary model to animal models for PD, with two main advantages, *i.e.,* being cost-efficient and having translational potential being derived from human iPSCs. Such models are especially useful for higher throughput screening of drugs and thus the discovery of new treatments (Pamies et al., 2014). The model was exposed to chemicals commonly used to induce PD-like symptoms both *in vivo* and *in vitro* (6-OHDA, MPTP, and MPP^+), since these chemicals are known to produce dopaminergic neuron loss *via* mechanisms likely involving oxidative stress and mitochondrial dysfunction. The concentrations used here were relatively high to observe toxic effects after short-term exposure of 24 h but are in line with other *in vitro* work (Zhao et al., 2017; Wu et al., 2017).

6-OHDA is a neurotoxic synthetic organic compound that is relatively selective for monoaminergic neurons due to the preferential uptake by dopamine and noradrenergic reuptake transporters (Blum et al., 2001). Upon entry into neurons, 6-OHDA accumulates in the cytosol and increases ROS levels. ROS production is induced by at least two different mechanisms, namely deamination by monoamine oxidase (MAO) or auto-oxidation (Breese and Traylor, 1971; Karoum et al., 1993). Excessive ROS can induce DNA damage, lipid peroxidation, and cytoskeleton disorganization that ultimately can lead to cell death (Blum et al., 2001). In our study, BrainSpheres exposed to increasing concentrations of 6-ODHA showed an increase in ROS and a decrease in cell viability and mitochondrial membrane potential (Fig. 2). We identified concentrations mainly affecting dopaminergic neurons using confocal images to assess specific effects on dopaminergic neurons without general neurotoxicity. Confocal images (Fig. 3) show how non-cytotoxic concentrations (100 and 500 μM) can disrupt selectively TH-positive cells without changing staining of the general neuronal marker NF200. In addition, genes related to oxidative stress (*GSTO1*, *SOD2*) were found to be upregulated after 6-OHDA treatment (500 μM) (Fig. 4A).

Another mechanism of 6-OHDA is the inhibition of mitochondrial complex I (Glinka and Youdim, 1995). Although, this is not considered the main mode of action, decrease in available ATP can induce cell death itself and cause alterations of the membrane potential (Lotharius et al., 1999) and disruption of complex I leads to parkinsonism in mice (González-Rodríguez et al., 2021). In this study, we found some evidence that 6-OHDA affects cellular energy pathways. Gene expression of the mitochondrial complex V (ATP synthase in mitochondria that produces ATP using the proton gradient generated by the respiratory chain) subunit *ATP5O* was significantly increased after 24 h treatment with 6-OHDA (Fig. 4A). Furthermore, the decrease of the extracellular metabolites D-glucose and creatine (Fig. 4B) indicates that 6-OHDA affects cellular metabolism and ATP production, either as primary or secondary effect. Gene expression of *KCMJ6* and *CALB1* were statistically down-regulated, indicating again a clear effect of 6-OHDA in dopaminergic neurons. However, transcription levels of the genes expressing the rate limiting enzyme of dopamine synthesis *(TH)* and of the dopamine transporter *(SLC6A3)* were significantly increased by 6-OHDA treatment. We speculate that the presence of 6-OHDA may trigger the upregulation of genes involved in dopamine production (TH) and transport (SLC6A3),

potentially a compensatory mechanism in the presence of oxidatively damaged dopamine. This effect was not observed for either MPTP or MPP^+. The upregulation of multiple dopamine-signaling elements specifically by 6-OHDA indicate that the tested compounds have different mode of actions. The possibility that the higher toxicity of 6-OHDA may partially be due to an increased dopamine metabolism and the associated enhanced metabolic stress (Blum et al., 2001) warrants further examination.

In vivo experiments of 6-OHDA-induced PD have several challenges. Since 6-OHDA does not cross the blood-brain barrier, it needs to be injected directly into the striatum or substantia nigra to deplete dopaminergic neurons and reproduce the pathophysiological characteristics of PD (Blum et al., 2001). After injection, the dopaminergic neurons degenerate within 24 h without showing apoptotic morphology. Exposure of BrainSpheres to 6-OHDA for 24 h resulted not only in an altered gene expression and a changed pattern of extracellular metabolites resembling those observed in PD (Fig. 4A and B) but also induced morphologic alterations of dopaminergic neurons as revealed by immunocytochemistry (Fig. 3 and Fig. 5A). Our BBB experiments showed that 6-OHDA disrupts the endothelial barrier and therefore eventually crosses the barrier and affects the BrainSpheres. A significant decrease in TEER (Fig. 5D) and increased endothelial cell area (Fig. 5C) indicate endothelial disruption. Even though it is believed that 6-OHDA normally does not cross the BBB, it has been shown to alter the BBB permeability in animals (Carvey et al., 2005; Wheeler et al., 2014), consistent with the observations here. However, the barrier established in this study is less complex than the BBB *in vivo* as it lacks several important cell types such as pericytes and astrocytes. Thus, the 6-OHDA model appears to largely reflect findings *in vivo* but without any noted improvements except the obvious ethical ones and higher throughput.

In contrast to 6-OHDA, MPTP is able to cross the BBB. However, it needs to be converted to its active form MPP^+ in order to induce PD-like symptoms (Blum et al., 2001). The enzyme MAO-B, mainly found in glial cells, converts MPTP into MPP^+ (Chiba et al., 1985). MPP^+ is transported into dopaminergic neurons *via* the dopamine transporter, where it accumulates (Chiba et al., 1985). If MPP^+ is excessive in the cytosol it enters the mitochondria by an energy-dependent mechanism (Ramsay et al., 1986), where it inhibits complex I that causes decreased ATP levels and subsequently leads to cell death (Blum et al., 2001).

The BrainSpheres model includes astrocytes (Pamies et al., 2016), therefore it is expected that MPTP can be converted into MPP^+ causing dopaminergic cell death. Using the current experimental set-up, we indeed observed PD-relevant alterations of ROS-levels and mitochondrial dysfunction, mainly at overall cytotoxic concentrations (Fig. 2). Nevertheless, immunocytochemistry and gene expression results (Figs. 3 and 4) provided evidence for MPTP-induced selective toxicity on dopaminergic neurons. The low level of effects might be attributed to the time needed to metabolize MPTP to MPP+ in comparison to the cultures where MPP+ was added. Also, the metabolic capacity of astrocytes needs to be studied further. Another possibility, why MPTP seemed to be less cytotoxic for BrainSpheres than the other tested compounds, can be a unique pattern of molecular regulations at the tested concentrations, selectively affecting dopaminergic neurons. While MPP^+ and 6-OHDA

resulted in a drop of creatine and extracellular D-glucose in the medium, and therefore may indicate an energy crisis, these effects were not observed for MPTP. Animal studies have recently shown a link between oligodendrocyte degeneration and MPTP exposure (Annese et al., 2013). MPTP crosses the BBB *in vivo* and in our transwell model, MPTP also crossed a monolayer of human brain microvascular endothelial cells and induced effects on the BrainSpheres (Fig. 5A and E). No effects were observed at the TEER by MPTP, indicating an intact barrier (Fig. 5D). However, the cell area of the endothelial cells was increased, suggesting toxicity also to these cells (Fig. 5C). Furthermore, in the present study an upregulation (not statistically significant) of the oligodendrocyte marker Olig2 five days after washout (Fig. 4D) was observed in the MPTP condition, which may have implications for Multiple Systems Atrophy, another synucleinopathy, characterized by pathology preferentially in oligodendrocytes (Krismer and Wenning, 2017). Thus, again the MPTP model appears to largely reflect findings *in vivo* but compared to other toxicants the metabolic activation seems to be limiting its effects.

Similar to very low concentrations of 6-OHDA (20 μM) we observed an apparent increase in cell viability at medium concentrations of MPTP (500 μM) (Fig. 2A), although this effect was not statistically significant. Possibly this could indicate protective adaptations of the cells in response to sub harmful cellular stress, leading to subsequent enhanced resilience. Such biphasic responses (beneficial at low, and detrimental at high concentrations) are referred to as hormesis (Ristow and Schmeisser, 2014; Esparza-Moltó et al., 2021). The recently described stimulating effect of the mitochondrial complex IV inhibitor cyanide on mitochondrial respiration with resulting increased cell proliferation is an example for a similar effect (Randi et al., 2021).

MPP^+ is used in many *in vitro* studies since it is the active metabolite of MPTP that induces PD-like effects (Blum et al., 2001). In this study, the cytotoxic concentration calculated by resazurin assay of MPP^+ was 1000 μM, with significant changes in the mitochondrial membrane potential at 500 μM (Fig. 2B). Statistically significant changes were found in gene expression of dopaminergic neuron selected genes KCMJ6 and CALB1 (Fig. 4A). However, these were the only genes that show to be affected after 1000 μM MPP+ exposure. Exposure to 1000 μM of MPP^+, induced morphological changes in dopaminergic neurons, detected by immunocytochemistry for TH, but also induced morphological changes in the general neuronal marker NF200 (Fig. 3), indicating a less specific effect. In contrast to 6-OHDA and MPTP, for which increased ROS-production was observed, MPP^+ was rather associated with a reduction in ROS, potentially due to high cell death. According to this observation, at the concentrations selected for gene expression experiments, components of REDOX-regulation systems (*GSTO1, SOD2* and/or *KEAP1*) were upregulated by 6-OHDA and MPTP, but not by MPP^+ (Fig. 4A). The relatively mild effects of MPP^+ even at high concentrations may be due to limitations of the acute exposure scheme and delayed effects may be observed at later time points. In fact, exposure to all compounds induced a significant down-regulation of the expression of *TH* five days later, after the compounds were washed out (Fig. 4C). Other genes not directly related with dopaminergic neurons were slightly modified after the wash-out period such as *GFAP* for 6-OHDA and *OLIG2* for MPTP (Fig. 4C). The use of the active metabolite of MPTP thus did not have evident advantages in the model and due to the presence of astrocytes seems not to be necessary.

4.1. Current limitations and perspectives

While the model employed in this study recapitulated PD-relevant molecular processes, numerous future modifications will have the potential to substantially increase the relevance of the BrainSphere model for PD even more. First, the possibility of personalization of the model by using PD-patient derived iPSCs, or by introducing PD-related mutations in the iPSCs, is a huge asset of this approach. The generation of such vulnerable iPSCs has been assessed in various studies as summarized recently (Fares et al., 2021). In addition, animal models of PD have several important short-comings to accurately model neurodegenerative processes in PD. In commonly used animal models for example the role of neuromelanin in the neuronal vulnerability in PD is usually not accounted for. There is no neuromelanin in rodent brain, but neuromelanin may be an important factor for neuronal vulnerability in PD (Hirsch et al., 1988). While efforts have been undertaken to generate rodent models that accumulate neuromelanin, *e.g.* by overexpression of human tyrosinase in rat substantia nigra (Carballo-Carbajal et al., 2019), these models presently are rarely used as PD models. In brain organoids neuromelanin can form spontaneously, as for example reported for brain organoids derived from three-dimensional differentiation of midbrain floor plate neural progenitor cells (Smits et al., 2019).

Recently, cell and animal models, in which PD-like processes are triggered *via* administration (usually intra-cerebral) of misfolded and aggregated alpha-synuclein have become very popular, because the slow pathogenesis is more accurately reflected in these models and the induced de-novo alpha-synuclein pathology resembles Lewy bodies in PD (Fares et al., 2021). The combination of BrainSpheres with such models in our opinion has great potential to both reduce the necessity of animal models and to increase the translational potential.

The integration of these aspects will make the BrainSphere model particularly suitable to study PD-related brain pathology. Taking advantage of the wealth of multi-omics data on PD (Schilder et al., 2022), it will allow the testing of precise questions, for example the genetic modulation of pathology-related genes, such as genes expressing antioxidant, mitochondrial- or lysosomal-functions associated genes.

Despite much ongoing research on and accumulating insights in PD pathogenesis, there are many fundamental open questions. One is the question about the causal role of specific molecular events in neurodegeneration; for example the contribution of mitochondrial dysfunctions, of alpha-synuclein pathology or the interaction of both (Burtscher et al., 2021). Another enigma is the role of cell-autonomous *versus* non-cell autonomous factors in selective neuronal vulnerability in PD (Surmeier, 2018; Gonzalez-Rodriguez et al., 2020). Due to the advantages of 3D organotypic model (derived from human iPSCs, therefore relevant for the human disease and genetically easily modifiable, increased complexity in comparison to other cellular models by inclusion of different cell-types and interactions and allowing the modeling of numerous pathological factors of PD pathogenesis, cost-effective compared to animal models), we think that this model can contribute in tackling those crucial questions.

5. Conclusions

In conclusion, our model in combination with commonly used compounds to induce PD-like phenotype, recapitulated several molecular alterations relevant for the disease, including ROS-formation, mitochondrial dysfunction and, most importantly, selective dopaminergic neuron vulnerability. This study indicates that the selected compounds have different pathological mechanisms (Fig. 6), which result in a similar outcome, *i.e.,* loss of dopaminergic neurons. The possibility to perform detailed investigations and comparisons of toxinmechanisms in a human iPSC model enables understanding the respective PD models and their translational potential.

6-OHDA was the most potent compound to induce dopaminergic neuronal effects in the human BrainSpheres. The effects on cellular functions by fluorescence assays, gene expression, and metabolites were observed at concentrations that did not induce general cytotoxicity. Moreover, images from immunocytochemistry show that 6-OHDA more specifically affects the dopaminergic neurons compared to MPTP and MPP^+. These findings suggest that 6-OHDA exposure in BrainSpheres is most suitable to reproduce results found in *in vivo* chemical-induced PD-like models. The specific effects on dopaminergic neurons after exposure to MPTP and MPP^+ were less pronounced and the exposure scenario likely needs to be optimized. The use of BrainSpheres enables faster and cheaper mechanistic analysis of these agents. The drastically improved throughput of the model compared to animal tests will allow specific aspects related to human and clinical relevance to be addressed more comprehensively. The 3D co-culture of different brain cells including glial cells in the BrainSpheres offers several advantages (Alepee et al., 2014), such as the direct comparison of dopaminergic neuron damage to other cell types, inter-cellular cooperation, *e.g.,* the activation of MPTP by astrocytes, and potential use to model pathologies in non-neuronal cell-types (*e.g.* in oligodendrocytes for Multiple Systems Atrophy). Furthermore, the further optimization of treatment protocols and the assessment of additional functional endpoints and biomarkers such as cytoplasmic inclusion bodies (Lewy bodies) promise to improve the relevance.

The problem of translating preclinical models to clinically successful drugs has been called a “valley of death” (Seyhan, 2019). The irrelevance of the disease models is of critical importance here. Reproducing an animal model that did not help *in vitro* does not improve usefulness if no value is added. Very often, the failure to select proper drug candidates is attributed to species differences as often discussed also for PD. Here, we demonstrate that we can recapitulate basic features of the animal models translating them to human 3D brain model. While we did not extend this work to any pharmacological interventions, some basic observations such as the need for extremely high doses and limited selectivity for dopaminergic neurons already challenge that mere translation to a human 3D brain model improves the situation. This does, however, not preclude that the use of stem cells from PD patients or healthy donors after introduction of risk genes by molecular biology with or without toxicants could result in more relevant human PD models. Thus, future variants of the model might be a useful tool to better understand the mechanisms of the disease and explore the use of new potential curative drugs.

Supplementary Material

Refer to Web version on PubMed Central for supplementary material.

Acknowledgment

This work was supported by NIH NCATS (grant U18TR000547 “A 3D Model of Human Brain Development for Studying Gene/Environment Interactions”, PIs Hartung and Hogberg) and Alternatives Research & Development Foundation (“A 3D in vitro ‘mini-brain’ model to study Parkinson’s disease”, PIs Hartung and Hogberg). International Foundation for Ethical Research Graduate Fellowship Funding provided to Georgina Harris.

References

Aguado J, Wolvetang EJ, 2022. Exploring aging interventions in human brain organoids. Aging (Albany NY) 14, 1592–1593. 10.18632/aging.203925. [PubMed: 35247254]

Alepee N, Bahinski A, Daneshian M, et al. , 2014. State-of-the-art of 3d cultures (organs-on-a-chip) in safety testing and pathophysiology. ALTEX 31, 441–477. 10.14573/altex1406111. [PubMed: 25027500]

Annese V, Barcia C, Ros-Bernal F, et al. , 2013. Evidence of oligodendrogliosis in 1-methyl-4-phenyl-1,2,3,6-tetrahydropyridine (mptp)-induced parkinsonism. Neuropathol. Appl. Neurobiol 39, 132–143. 10.1111/j.1365-2990.2012.01271.x. [PubMed: 22443457]

Aquilano K, Baldelli S, Ciriolo MR, 2014. Glutathione: new roles in redox signaling for an old antioxidant. Front. Pharmacol 5 10.3389/fphar.2014.00196.

Bedard C, Wallman MJ, Pourcher E, et al. , 2011. Serotonin and dopamine striatal innervation in parkinson’s disease and huntington’s chorea. Parkinsonism Relat. Disord 17, 593–598. 10.1016/j.parkreldis.2011.05.012. [PubMed: 21664855]

Bezard E, Yue Z, Kirik D, et al. , 2013. Animal models of parkinson’s disease: limits and relevance to neuroprotection studies. Mov. Disord 28, 61–70. 10.1002/mds.25108. [PubMed: 22753348]

Bjorklund O, Shang M, Tonazzini I, et al. , 2008. Adenosine a1 and a3 receptors protect astrocytes from hypoxic damage. Eur. J. Pharmacol 596, 6–13. 10.1016/j.ejphar.2008.08.002. [PubMed: 18727925]

Blesa J, Foffani G, Dehay B, et al. , 2022. Motor and non-motor circuit disturbances in early parkinson disease: which happens first? Nat. Rev. Neurosci 23, 115–128. 10.1038/s41583-021-00542-9. [PubMed: 34907352]

Blum D, Torch S, Lambeng N, et al. , 2001. Molecular pathways involved in the neurotoxicity of 6-ohda, dopamine and mptp: contribution to the apoptotic theory in parkinson’s disease. Prog. Neurobiol 65, 135–172. [PubMed: 11403877]

Boucherie DM, Duarte GS, Machado T, et al. , 2021. Parkinson’s disease drug development since 1999: a story of repurposing and relative success. J. Parkinsons Dis 11, 421–429. 10.3233/Jpd-202184. [PubMed: 33459662]

Breese GR, Traylor TD, 1971. Depletion of brain noradrenaline and dopamine by 6-hydroxydopamine. Br. J. Pharmacol 42, 88–99. [PubMed: 5580702]

Burtscher J, Syed MMK, Keller MA, et al. , 2021. Fatal attraction - the role of hypoxia when alpha-synuclein gets intimate with mitochondria. Neurobiol. Aging 107, 128–141. 10.1016/j.neurobiolaging.2021.07.017. [PubMed: 34428721]

Carballo-Carbajal I, Laguna A, Romero-Giménez J, et al. , 2019. Brain tyrosinase overexpression implicates age-dependent neuromelanin production in parkinson’s disease pathogenesis. Nat. Commun 10, 973. 10.1038/s41467-019-08858-y. [PubMed: 30846695]

Carlsson T, Carta M, Winkler C, et al. , 2007. Serotonin neuron transplants exacerbate l-dopa-induced dyskinesias in a rat model of parkinson’s disease. J. Neurosci 27, 8011–8022. 10.1523/JNEUROSCI.2079-07.2007. [PubMed: 17652591]

Carvey PM, Zhao CH, Hendey B, et al. , 2005. 6-hydroxydopamine-induced alterations in blood-brain barrier permeability. Eur. J. Neurosci 22, 1158–1168. 10.1111/j.1460-9568.2005.04281.x. [PubMed: 16176358]

Chang Y, Kim J, Park H, et al. , 2020. Modelling neurodegenerative diseases with 3d brain organoids. Biol. Rev. Camb. Philos. Soc 95, 1497–1509. 10.1111/brv.12626. [PubMed: 32568450]

Chesnut M, Hartung T, Hogberg H, et al. , 2021. Human oligodendrocytes and myelin in vitro to evaluate developmental neurotoxicity. Int. J. Mol. Sci 22 10.3390/ijms22157929.

Chiba K, Trevor AJ, Castagnoli N Jr., 1985. Active uptake of mpp+, a metabolite of mptp, by brain synaptosomes. Biochem. Biophys. Res. Commun 128, 1228–1232. 10.1016/0006-291x(85)91071-x. [PubMed: 3873939]

Chou BK, Mali P, Huang XS, et al. , 2011. Efficient human ips cell derivation by a non-integrating plasmid from blood cells with unique epigenetic and gene expression signatures. Cell Res. 21, 518–529. 10.1038/cr.2011.12. [PubMed: 21243013]

Covarrubias L, Hernandez-Garcia D, Schnabel D, et al. , 2008. Function of reactive oxygen species during animal development: passive or active? Dev. Biol 320, 1–11. 10.1016/j.ydbio.2008.04.041. [PubMed: 18555213]

Daneshian M, Busquet F, Hartung T, et al. , 2015. Animal use for science in europe. ALTEX 32, 261–274. 10.14573/altex.1509081. [PubMed: 26536288]

Dauer W, Przedborski S, 2003. Parkinson's disease: mechanisms and models. Neuron 39, 889–909. [PubMed: 12971891]

Esparza-Moltó PB, Romero-Carramiñana I, Núñez de Arenas C, et al. , 2021. Generation of mitochondrial reactive oxygen species is controlled by atpase inhibitory factor 1 and regulates cognition. PLoS Biol. 19, e3001252 10.1371/journal.pbio.3001252. [PubMed: 33983919]

Faivre F, Joshi A, Bezard E, et al. , 2019. The hidden side of parkinson's disease: studying pain, anxiety and depression in animal models. Neurosci. Biobehav. Rev 96, 335–352. 10.1016/j.neubiorev.2018.10.004. [PubMed: 30365972]

Fares MB, Jagannath S, Lashuel HA, 2021. Reverse engineering lewy bodies: how far have we come and how far can we go? Nat. Rev. Neurosci 22, 111–131. 10.1038/s41583-020-00416-6. [PubMed: 33432241]

Fiorenzano A, Sozzi E, Birtele M, et al. , 2021. Single-cell transcriptomics captures features of human midbrain development and dopamine neuron diversity in brain organoids. Nat. Commun 12, 7302. 10.1038/s41467-021-27464-5. [PubMed: 34911939]

Fisher MT, 2006. Proline to the rescue. Proc. Natl. Acad. Sci. U. S. A 103, 13265–13266. 10.1073/pnas.0606106103. [PubMed: 16938858]

Fredholm BB, Chen JF, Masino SA, et al. , 2005. Actions of adenosine at its receptors in the cns: insights from knockouts and drugs. Annu. Rev. Pharmacol. Toxicol 45, 385–412. [PubMed: 15822182]

Glinka YY, Youdim MB, 1995. Inhibition of mitochondrial complexes i and iv by 6-hydroxydopamine. Eur. J. Pharmacol 292, 329–332. [PubMed: 7796873]

Gonzalez-Rodriguez P, Zampese E, Surmeier DJ, 2020. Selective neuronal vulnerability in parkinson's disease. Prog. Brain Res 252, 61–89. [PubMed: 32247375]

González-Rodríguez P, Zampese E, Stout KA, et al. , 2021. Disruption of mitochondrial complex i induces progressive parkinsonism. Nature 599, 650–656. 10.1038/s41586-021-04059-0. [PubMed: 34732887]

Halliwell B, 1991. Reactive oxygen species in living systems: source, biochemistry, and role in human disease. Am. J. Med 91, 14S–22S. 10.1016/0002-9343(91)90279-7.

Hirsch E, Graybiel AM, Agid YA, 1988. Melanized dopaminergic neurons are differentially susceptible to degeneration in parkinson's disease. Nature 334, 345–348. [PubMed: 2899295]

Hirsch EC, Faucheux B, Damier P, et al. , 1997. Neuronal vulnerability in parkinson's disease. J. Neural Transm Suppl. 50, 79–88.

Hou Y, Dan X, Babbar M, et al. , 2019. Ageing as a risk factor for neurodegenerative disease. Nat. Rev. Neurol 15, 565–581. 10.1038/s41582-019-0244-7. [PubMed: 31501588]

Ibanez P, Bonnet AM, Debarges B, et al. , 2004. Causal relation between alpha-synuclein gene duplication and familial parkinson's disease. Lancet 364, 1169–1171. 10.1016/s0140-6736(04)17104-3. [PubMed: 15451225]

Jagmag SA, Tripathi N, Shukla SD, et al. , 2016. Evaluation of models of parkinson's disease. Front. Neurosci 9 10.3389/fnins.2015.00503.

Jeon BS, Jackson-Lewis V, Burke RE, 1995. 6-hydroxydopamine lesion of the rat substantia nigra: time course and morphology of cell death. Neurodegeneration 4, 131–137. [PubMed: 7583676]

Jo J, Xiao Y, Sun AX, et al. , 2016. Midbrain-like organoids from human pluripotent stem cells contain functional dopaminergic and neuromelanin-producing neurons. Cell Stem Cell 19, 248–257. 10.1016/j.stem.2016.07.005. [PubMed: 27476966]

Kalia LV, Kalia SK, Lang AE, 2015. Disease-modifying strategies for parkinson's disease. Mov. Disord 30, 1442–1450. 10.1002/mds.26354. [PubMed: 26208210]

Karoum F, Chrapusta SJ, Egan MF, et al. , 1993. Absence of 6-hydroxydopamine in the rat brain after treatment with stimulants and other dopaminergic agents: a mass fragmentographic study. J. Neurochem 61, 1369–1375. [PubMed: 8104232]

Katt ME, Xu ZS, Gerecht S, et al. , 2016. Human brain microvascular endothelial cells derived from the bc1 ips cell line exhibit a blood-brain barrier phenotype. PLoS One 11. 10.1371/journal.pone.0152105.

Krismer F, Wenning GK, 2017. Multiple system atrophy: insights into a rare and debilitating movement disorder. Nat. Rev. Neurol 13, 232–243. 10.1038/nrneurol.2017.26. [PubMed: 28303913]

Krug AK, Gutbier S, Zhao L, et al. , 2014. Transcriptional and metabolic adaptation of human neurons to the mitochondrial toxicant mpp(+). Cell Death Dis. 5, e1222 10.1038/cddis.2014.166. [PubMed: 24810058]

Kruger R, Kuhn W, Muller T, et al. , 1998. Ala30pro mutation in the gene encoding alpha-synuclein in parkinson's disease. Nat. Genet 18, 106–108. 10.1038/ng0298-106. [PubMed: 9462735]

Lashuel HA, Overk CR, Oueslati A, et al. , 2013. The many faces of α-synuclein: from structure and toxicity to therapeutic target. Nat. Rev. Neurosci 14, 38–48. [PubMed: 23254192]

Le W, Sayana P, Jankovic J, 2014. Animal models of parkinson's disease: a gateway to therapeutics? Neurotherapeutics 11, 92–110. 10.1007/sl3311013-0234-1. [PubMed: 24158912]

Lee CS, Schulzer M, Mak EK, et al. , 1994. Clinical observations on the rate of progression of idiopathic parkinsonism. Brain 117 (Pt 3), 501–507. [PubMed: 8032860]

Li S, Yu Q, Lu X, et al. , 2009. Determination of d,l-serine in midbrain of parkinson's disease mouse by capillary electrophoresis with in-column light-emitting diode induced fluorescence detection. J. Sep. Sci 32, 282–287. 10.1002/jssc.200800459. [PubMed: 19156646]

Lotharius J, Dugan LL, O'Malley KL, 1999. Distinct mechanisms underlie neurotoxin-mediated cell death in cultured dopaminergic neurons. J. Neurosci 19, 1284–1293. [PubMed: 9952406]

Maertens A, Bouhifd M, Zhao L, et al. , 2017. Metabolomic network analysis of estrogen-stimulated mcf-7 cells: a comparison of overrepresentation analysis, quantitative enrichment analysis and pathway analysis versus metabolite network analysis. Arch. Toxicol 91, 217–230. 10.1007/s00204-016-1695-x. [PubMed: 27039105]

Marinus J, Zhu K, Marras C, et al. , 2018. Risk factors for non-motor symptoms in parkinson's disease. Lancet Neurol. 17, 559–568. 10.1016/s1474-4422(18)30127-3. [PubMed: 29699914]

Meininger V, Flamier A, Phan T, et al. , 1982. L-methionine treatment of parkinson's disease: preliminary results. Rev. Neurol. (Paris) 138, 297–303. [PubMed: 7134722]

Modafferi S, Zhong XL, Kleensang A, et al. , 2021. Gene-environment interactions in developmental neurotoxicity: a case study of synergy between chlorpyrifos and chd8 knockout in human brainspheres. Environ. Health Perspect 129 10.1289/Ehp8580.

Monzio Compagnoni G, Di Fonzo A, Corti S, et al. , 2020. The role of mitochondria in neurodegenerative diseases: the lesson from alzheimer's disease and parkinson's disease. Mol. Neurobiol 57, 2959–2980. [PubMed: 32445085]

O'Brien J, Pognan F, 2001. Investigation of the alamar blue (resazurin) fluorescent dye for the assessment of mammalian cell cytotoxicity. Toxicology 164, 132.

Pamies D, Hartung T, 2017. 21st century cell culture for 21st century toxicology. Chem. Res. Toxicol 30, 43–52. 10.1021/acs.chemrestox.6b00269. [PubMed: 28092941]

Pamies D, Hartung T, Hogberg HT, 2014. Biological and medical applications of a brain-on-a-chip. Exp. Biol. Med 239, 1096–1107. 10.1177/1535370214537738.

Pamies D, Barreras P, Block K, et al. , 2016. A human brain microphysiological system derived from induced pluripotent stem cells to study neurological diseases and toxicity. ALTEX. 10.14573/altex.1609122.

Pamies D, Block K, Lau P, et al. , 2018. Rotenone exerts developmental neurotoxicity in a human brain spheroid model. Toxicol. Appl. Pharmacol 354, 101–114. 10.1016/j.taap.2018.02.003. [PubMed: 29428530]

Pamies D, Zurich MG, Hartung T, 2020. Organotypic models to study human glioblastoma: Studying the beast in its ecosystem. iScience 23, 101633. 10.1016/j.isci.2020.101633. [PubMed: 33103073]

Pamies D, Leist M, Coecke S, et al. , 2022. Guidance document on good cell and tissue culture practice 2.0 (gccp 2.0). ALTEX 39, 30–70. 10.14573/altex.2111011. [PubMed: 34882777]

Paredes-Rodriguez E, Vegas-Suarez S, Morera-Herreras T, et al. , 2020. The noradrenergic system in parkinson's disease. Front. Pharmacol 11, 435. 10.3389/fphar.2020.00435. [PubMed: 32322208]

Plummer S, Wallace S, Ball G, et al. , 2019. A human ipsc-derived 3d platform using primary brain cancer cells to study drug development and personalized medicine. Sci. Rep 9 10.1038/s41598-018-38130-0.

Polymeropoulos MH, Lavedan C, Leroy E, et al. , 1997. Mutation in the alpha-synuclein gene identified in families with parkinson's disease. Science 276, 2045–2047. [PubMed: 9197268]

Ramsay RR, Dadgar J, Trevor A, et al. , 1986. Energy-driven uptake of n-methyl-4-phenylpyridine by brain mitochondria mediates the neurotoxicity of mptp. Life Sci. 39, 581–588. 10.1016/0024-3205(86)90037-8. [PubMed: 3488484]

Randi EB, Zuhra K, Pecze L, et al. , 2021. Physiological concentrations of cyanide stimulate mitochondrial complex iv and enhance cellular bioenergetics. Proc. Natl. Acad. Sci. U. S. A 118 10.1073/pnas.2026245118.

Renner H, Grabos M, Becker KJ, et al. , 2020. A fully automated high-throughput workflow for 3d-based chemical screening in human midbrain organoids. Elife 9. 10.7554/eLife.52904.

Reyes S, Fu Y, Double K, et al. , 2012. Girk2 expression in dopamine neurons of the substantia nigra and ventral tegmental area. J. Comp. Neurol. 520, 2591–2607. 10.1002/cne.23051. [PubMed: 22252428]

Ristow M, Schmeisser K, 2014. Mitohormesis: promoting health and lifespan by increased levels of reactive oxygen species (ros). Dose-Resp. Publicat. Int. Hormesis Soc 12, 288–341. 10.2203/dose-response.13-035.Ristow.

Schilder BM, Navarro E, Raj T, 2022. Multi-omic insights into parkinson's disease: from genetic associations to functional mechanisms. Neurobiol. Dis 163, 105580 10.1016/j.nbd.2021.105580. [PubMed: 34871738]

Schmidt DE, Ebert MH, Lynn JC, et al. , 1997. Attenuation of 1-methyl-4-phenyl-pyridinium (mpp+) neurotoxicity by deprenyl in organotypic canine substantia nigra cultures. J. Neural Transm. (Vienna) 104, 875–885. 10.1007/BF01285555. [PubMed: 9451719]

Seyhan AA, 2019. Lost in translation the challenges with the use of animal models in translational research. Handbook of Biomarkers and Precision Medicine 36–43. 10.1201/9780429202872.

Sies H, Jones DP, 2020. Reactive oxygen species (ros) as pleiotropic physiological signalling agents. Nat. Rev. Mol. Cell Biol 1–21. [PubMed: 31676888]

Sies H, Belousov VV, Chandel NS, et al. , 2022. Defining roles of specific reactive oxygen species (ros) in cell biology and physiology. Nat. Rev. Mol. Cell Biol 10.1038/s41580-022-00456-z.

Singleton AB, Farrer M, Johnson J, et al. , 2003. Alpha-synuclein locus triplication causes parkinson's disease. Science 302, 841. 10.1126/science.1090278. [PubMed: 14593171]

Smits LM, Reinhardt L, Reinhardt P, et al. , 2019. Modeling parkinson's disease in midbrain-like organoids. NPJ Parkinsons Dis 5, 5. 10.1038/s41531-019-0078-4. [PubMed: 30963107]

Spillantini MG, Schmidt ML, Lee VM, et al. , 1997. Alpha-synuclein in lewy bodies. Nature 388, 839–840. 10.1038/42166. [PubMed: 9278044]

Surmeier DJ, 2018. Determinants of dopaminergic neuron loss in parkinson's disease. FEBS J. 285, 3657–3668. 10.1111/febs.14607. [PubMed: 30028088]

Tieu K, 2011. A guide to neurotoxic animal models of parkinson's disease. Cold Spring Harbor Perspect. Med 1, a009316.

Vingill S, Connor-Robson N, Wade-Martins R, 2018. Are rodent models of parkinson's disease behaving as they should? Behav. Brain Res 352, 133–141. 10.1016/j.bbr.2017.10.021. [PubMed: 29074404]

Wen Z, Nguyen HN, Guo Z, et al. , 2014. Synaptic dysregulation in a human ips cell model of mental disorders. Nature 515, 414–418. 10.1038/nature13716. [PubMed: 25132547]

Wheeler CJ, Seksenyan A, Koronyo Y, et al. , 2014. T-lymphocyte deficiency exacerbates behavioral deficits in the 6-ohda unilateral lesion rat model for parkinson's disease. J Neurol Neurophysiol 5. 10.4172/2155-9562.1000209.

Wong YC, Krainc D, 2017. Alpha-synuclein toxicity in neurodegeneration: mechanism and therapeutic strategies. Nat. Med 23, 1–13. 10.1038/nm.4269.

Wong AD, Ye M, Levy AF, et al. , 2013. The blood-brain barrier: An engineering perspective. Front Neuroeng 6, 7. 10.3389/fneng.2013.00007. [PubMed: 24009582]

Wu L, Du ZR, Xu AL, et al. , 2017. Neuroprotective effects of total flavonoid fraction of the epimedium koreanum nakai extract on dopaminergic neurons: in vivo and in vitro. Biomed. Pharmacother 91, 656–663. 10.1016/j.biopha.2017.04.083. [PubMed: 28494419]

Yeo S, An KS, Hong YM, et al. , 2015. Neuroprotective changes in degeneration-related gene expression in the substantia nigra following acupuncture in an mptp mouse model of parkinsonism: microarray analysis. Genet. Mol. Biol 38, 115–127. 10.1590/S1415-475738120140137. [PubMed: 25983633]

Zander NE, Piehler T, Hogberg H, et al. , 2017. Explosive blast loading on human 3d aggregate minibrains. Cell. Mol. Neurobiol 37, 1331–1334. 10.1007/s10571-017-0463-7. [PubMed: 28110483]

Zarranz JJ, Alegre J, Gomez-Esteban JC, et al. , 2004. The new mutation, e46k, of alpha-synuclein causes parkinson and lewy body dementia. Ann. Neurol 55, 164–173. 10.1002/ana.10795. [PubMed: 14755719]

Zhao L, Feng Y, Shi A, et al. , 2017. Neuroprotective effect of low-intensity pulsed ultrasound against mpp+−induced neurotoxicity in pc12 cells: involvement of k2p channels and stretch-activated ion channels. Ultrasound Med. Biol 10.1016/j.ultrasmedbio.2017.04.020.

Zhong X, Harris G, Smirnova L, et al. , 2020. Antidepressant paroxetine exerts developmental neurotoxicity in an ipsc-derived 3d human brain model. Front. Cell. Neurosci 14, 25. 10.3389/fncel.2020.00025. [PubMed: 32153365]

Zhou QJ, Nino DF, Yamaguchi Y, et al. , 2021. Necrotizing enterocolitis induces t lymphocyte-mediated injury in the developing mammalian brain. Sci. Transl. Med 13 10.1126/scitranslmed.aay6621.

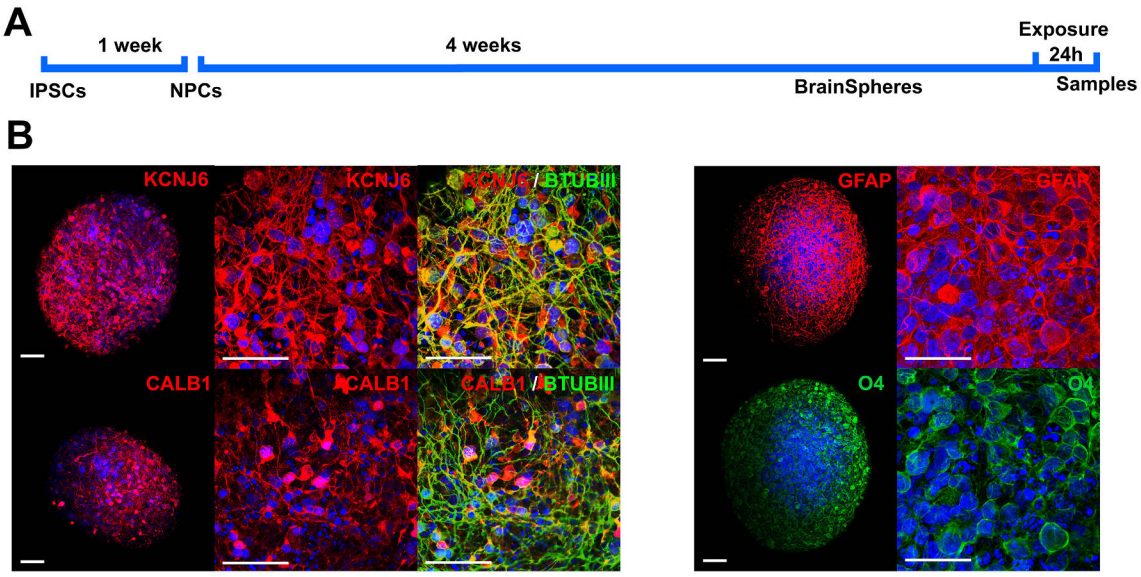

Fig. 1.

Experimental design and BrainSpheres characterization. A) shows diagram of experimental procedure described in material and methods. B) shows confocal images of neuronal marker BTUBIII, dopaminergic neurons markers (KCNJ6, CALB1), astrocytes marker (GFAP) and oligodendrocyte marker (O4). Bars represent 50 μm.

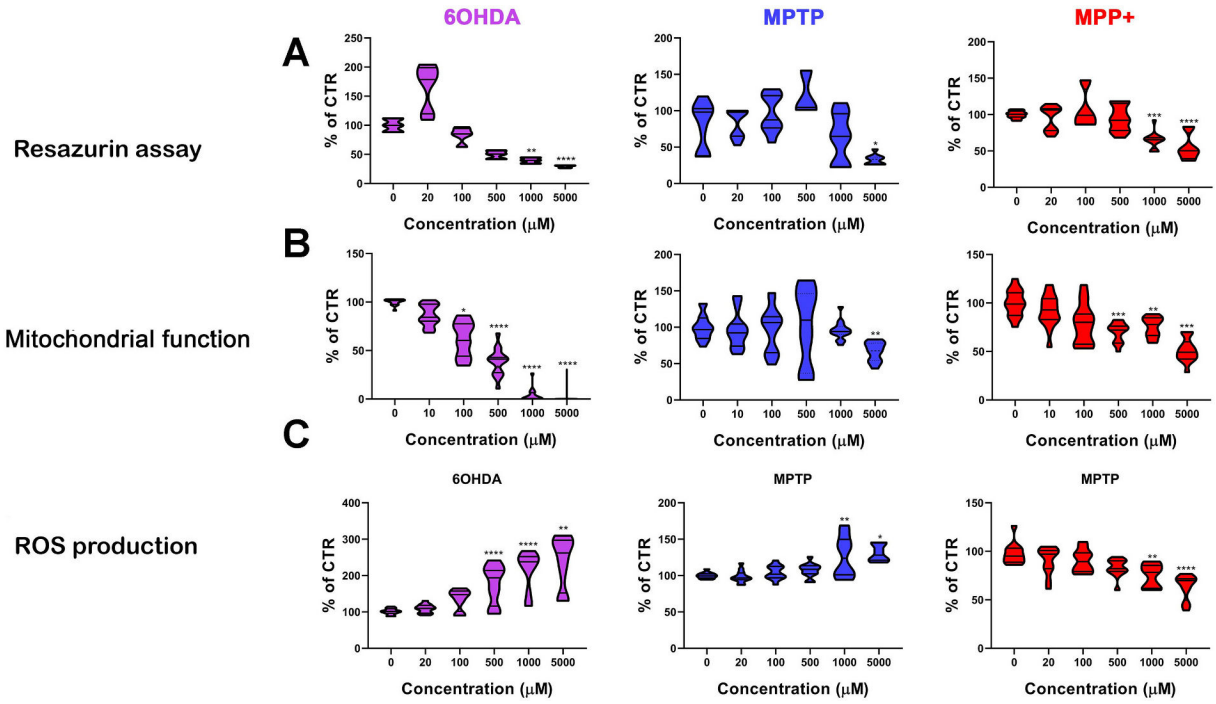

Fig. 2.

Effects of 24 h exposure to 6-OHDA, MPTP, and MPP^+ on (A) cell viability, (B) mitochondrial function, and (C) ROS production in 4 weeks differentiated BrainSpheres. BrainSpheres were treated with different concentrations of 6-OHDA, MPTP, and MPP^+ at 4 weeks of differentiation. Data is presented as percentage of control. One-Way ANOVA followed by Kruskal–Wallis multiple comparison H tests was performed to evaluate statistical significance *vs.* untreated controls (* $p < 0.05$, ** $p < 0.005$, *** $p < 0.0005$, **** $P < 0.0001$) in three independent experiments with 3 to 6 biological replicates per experiment.

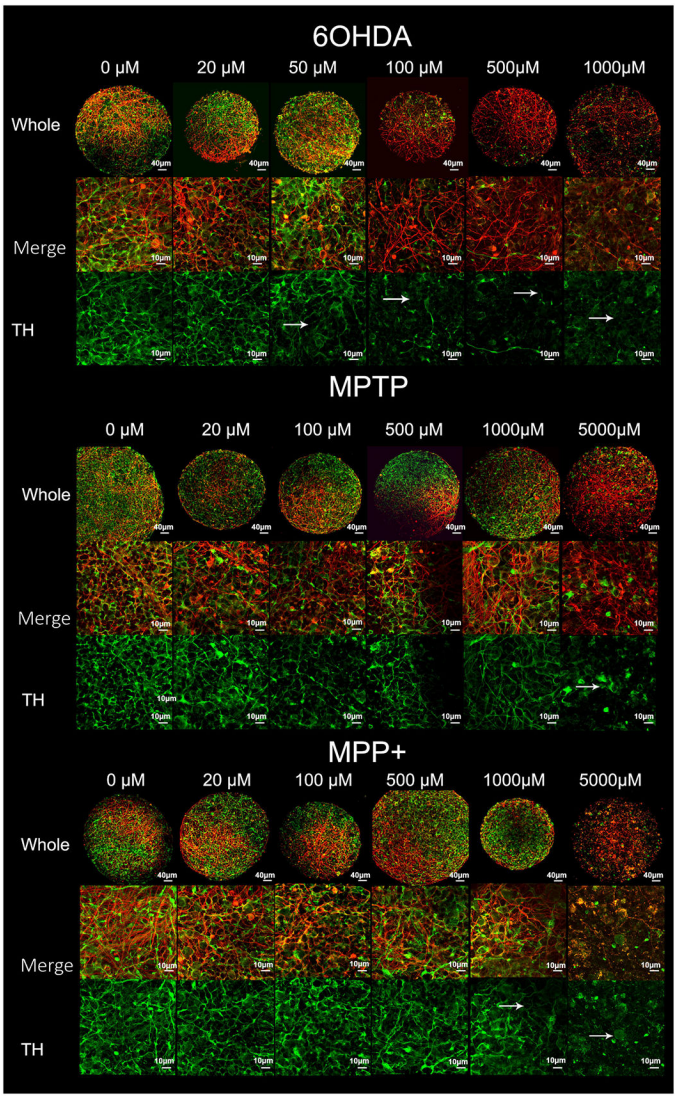

Fig. 3.

Selective degeneration of tyrosine hydroxylase (TH)-positive dopaminergic neurons after 24 h exposure to 6-OHDA, MPTP or MPP^+. Spheres were stained with thyrosine hydroxylase-specific antibody (TH, green) and anti-neurofilament antibody (NF200, red). From top to bottom shown of each codition: TH^+ and $NF200^+$ merged in whole BrainSpheres, 63× magnification of merge imagens and TH^+ alone. Values on top of each figure represents the concentration in µM. Arrows showing altered dopaminergic neurons morphology. Scale Bars represent 40 µm or 10 µm as indicated.

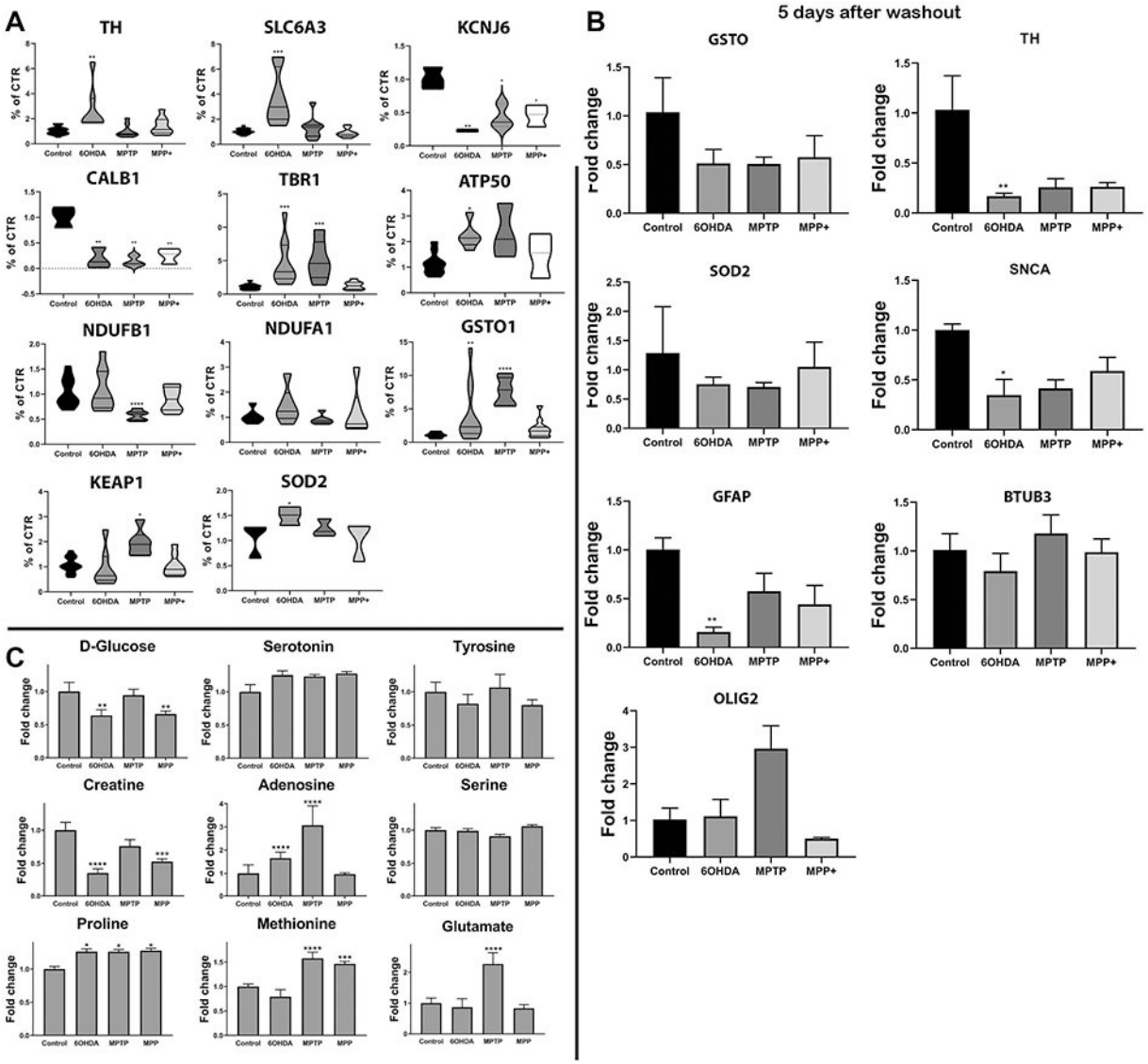

Fig. 4.

Alteration in expression of dopaminergic neurons- and oxidative stress-related genes and extracellular levels of metabolites after 24 h treatment of BrainSpheres with 6-OHDA (500 μM), MPTP (5000 μM) and MPP^+ (1000 μM). Gene expression of markers for dopaminergic neurons (*TH, SLC6A3, CALB1, KCNJ6, TBR*1), mitochondrial metabolism (*ATP5O, NDUFB1, NDUFA1*) and oxidative stress (*GSTO1, KEAP1, SOD2*) was analyzed by real-time qPCR. B) Extracellular metabolites measured by mass spectrometry (LC-MS/MS). C) Gene expression after compound washout and 5 days recovery period. In B and C bars represent mean ± SEM of 3–4 independent experiments. One-Way ANOVA followed by Kruskal–Wallis multiple comparison H tests was performed to evaluate statistical significance (* $p < 0.05$, ** $p < 0.005$, *** $p < 0.0005$, **** $P < 0.0001$).

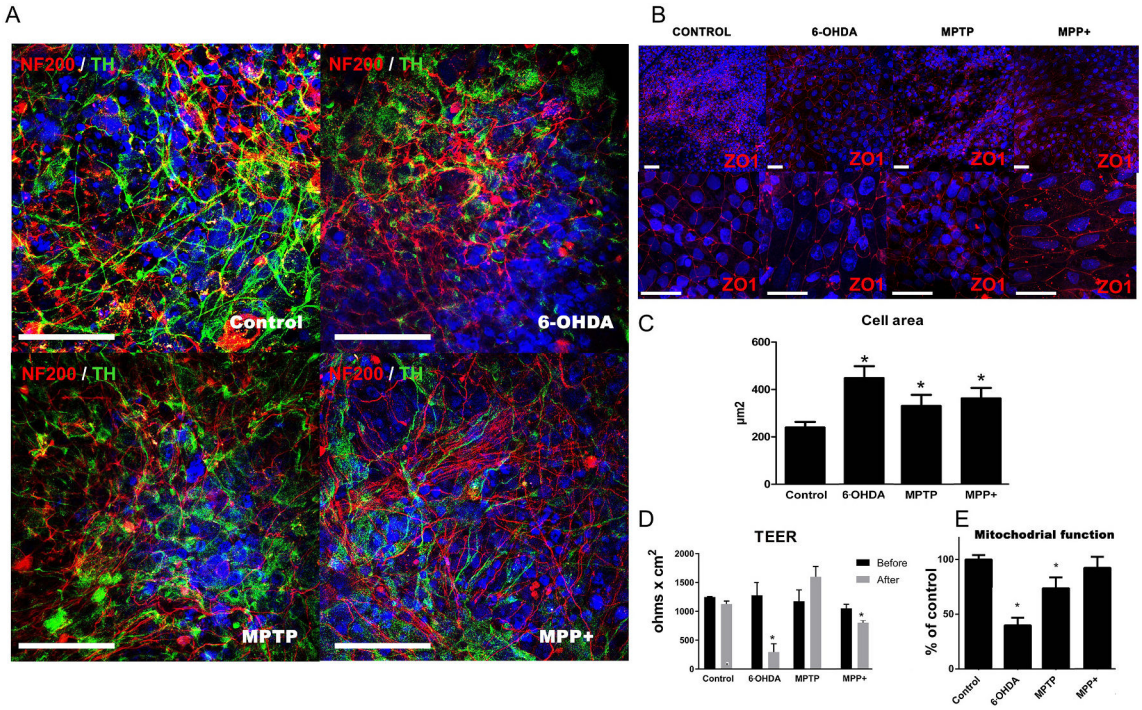

Fig. 5.

Blood Brain Barrier (BBB) incorporation to the BrainSpheres. BrainSpheres were cultured in the basal chamber while iPSC derived endothelial cells were cultured apically on the transwell membrane building a barrier between the upper and lower chambers. Chemicals (500 µM 6-OHDA, 5000 µM MPTP, or 1000 µM MPP^+) were added apically for 24 h. A) Immunocytochemistry for dopaminergic marker (TH, green), axonal marker (NF200, red). B) Immunocytochemistry for Tight junction protein 1 (ZO1, red) nuclei (blue). C) Cell area quantification of endothelial cells based on ZO1 staining D) TEER measurements after 24 h chemical exposure. E) Mitochondrial function in BrainSpheres after 24 h exposure measured by Mitotracker. Nuclei were stained with Hoechst. Bars represent 50 µm. Data represent mean ± SEM ($n = 3$). One-Way ANOVA followed by Kruskal–Wallis multiple comparison H tests was performed to evaluate statistical significance (* $p < 0.05$).

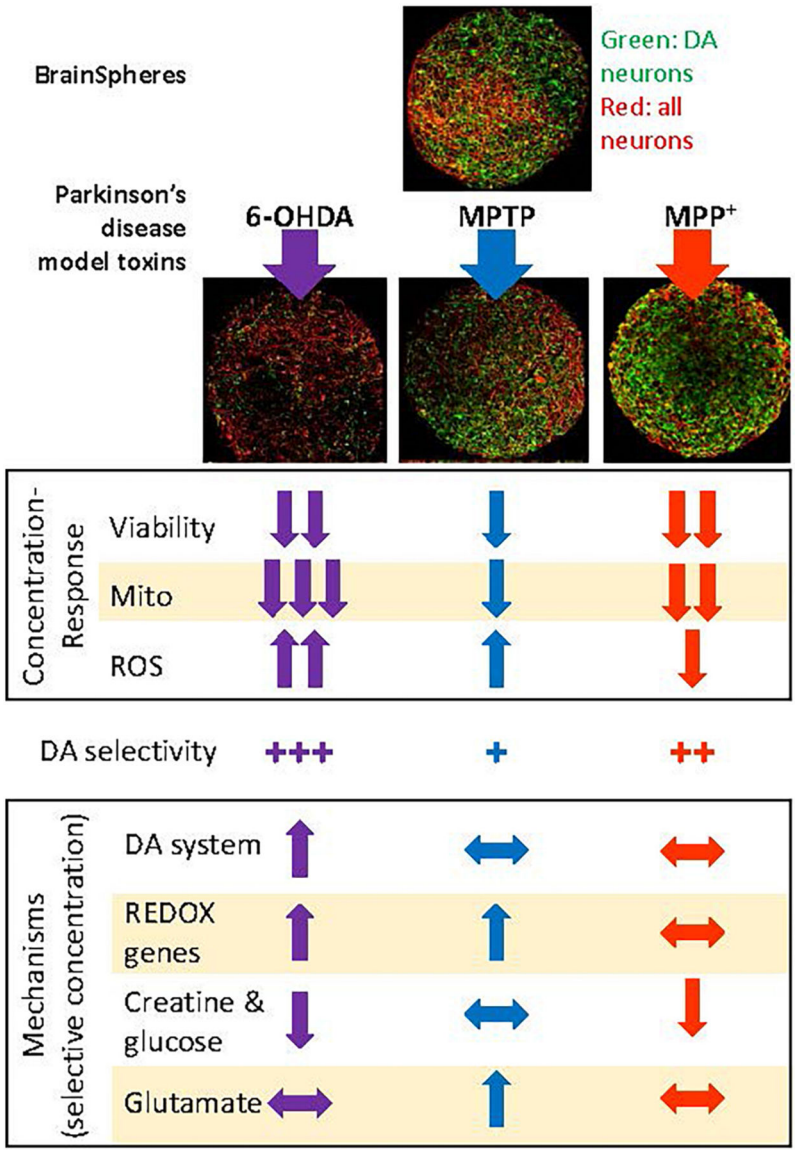

Fig. 6.

Differential effects of 6-OHDA, MPTP and MPP^+ on 4 weeks differentiated BrainSpheres. In concentration response experiments 6-OHDA was identified as most potent and with most selective effects on dopaminergic (DA) neurons, overall neuronal loss, mitochondrial (Mito) function and reactive oxygen species (ROS) generation compared to the other compounds. Arrows represent increase ↑, drease ↓ or no changes ↔ of the parameter studied.

Table 1

List of primers and associated genes used in RT-qPCR.

full name	abbreviation	primer number
Synuclein, alpha	*SNCA,*	Hs01103383
Solute carrier family 6 (neurotransmitter transporter), member 3	*SLC6A3*	Hs00997364
T-box, brain, 1	*TBR1*	Hs00232429
tyrosine hydroxylase	*TH*	Hs00165941
Calbindin 1	*CALB1*	Hs01077197
Potassium Inwardly Rectifying Channel Subfamily J Member 6	*KCNJ6*	Hs01040524
glutathione S-transferase omega 1	*GSTO1*	Hs02383465
Kelch-like ECH-associated protein 1	*KEAP1*	Hs00202227
superoxide dismutase 2	*SOD2*	Hs00167309
ATP synthase, H+ transporting, mitochondrial F1 complex, gamma polypeptide 1	*ATP5C1*	Hs01101219
ATP synthase, H+ transporting, mitochondrial F1 complex, O subunit	*ATP5O*	Hs00426889
NADH dehydrogenase (ubiquinone) 1 alpha subcomplex, 1	*NDUFA1*	Hs00244980
NADH dehydrogenase (ubiquinone) 1 beta subcomplex, 1	*NDUFB1*	Hs00929425
Glial fibrillary acidic protein	*GFAP*	Hs00909233
High class III beta-tubulin	*BTUBIII*	Hs00801390
Oligodendrocyte transcription factor	*OLIG2*	Hs00300164

Table 2

Selection of concentrations with selective dopaminergic neuron (DA) toxicity.

	Compounds		
Ratings	**6-OHDA**	**MPTP**	**MPP^+**
DA toxicity			
➔First indications of compromised DA neuron integrity (diffuse TH^+ staining)	≥ 50 μM	≥ 5000 μM	≥ 1000 μM
➔DA neurite loss	≥ 50 μM	≥ 5000 μM	≥ 1000 μM
➔Loss of majority of DA neurons	≥ 100 μM	≥ 5000 μM	≥ 5000 μM
General neuronal loss ($NF200^+$)	≥ 1000 μM	> 5000 μM	≥ 5000 μM
Rating for DA toxicity selectivity	+++	+	++
Selective DA toxicity; optimal window	500 μM	5000 μM	1000 μM